PHYSICAL REVIEW B VOLUME 16, NUMBER 9 1 NOVEMBER 1977

Electron-nuclear double resonance of V_{OD} defects in SrO†

J. L. Boldu O.,* H. J. Stapleton,‡ Y. Chen, and M. M. Abraham
Solid State Division, Oak Ridge National Laboratory, Oak Ridge, Tennessee 37830

(Received 13 June 1977)

Single crystals of SrO doped with deuterium were grown by the submerged-arc fusion technique. The V_{OD} center was produced by γ irradiation at 77 K and its identity confirmed by EPR and electron-nuclear double-resonance measurements. The defect possesses $\langle 100 \rangle$ axial symmetry and can be described with the spin-Hamiltonian parameters: $g_{\parallel} = 2.0013(2)$, $g_{\perp} = 2.0751(2)$, $A_{\parallel} = +0.396(2)$ MHz, $A_{\perp} = -0.195(2)$ MHz, and $P = +0.158(1)$ MHz. Absolute signs are based on the assumption that the reported positive deuterium nuclear moment requires the anisotropic portion of the hyperfine interaction to be positive. From the hyperfine parameters, a value of 5.078 Å for the OD^--(Sr vacancy)-O^- distance in this linear defect can be computed. Since the normal oxygen spacing in SrO is 5.16 Å, this implies an inward relaxation of the oxygens that is contrary to the previously observed cases of V_{OH} and V_{OD} defects in the alkaline-earth oxides where outward distortions occur.

I. INTRODUCTION

The production of V-type trapped-hole defects caused by ionizing irradiation in the alkaline-earth oxides MgO, CaO, and SrO and the study of their properties has been the subject of much recent research. (See review articles, Refs. 1–3.) The simplest of the V-type defects is the V^- center which is a cation vacancy with a positive hole trapped at a neighboring anion site (an O^- ion). Variations of the V^- center result from the addition of various impurity ions occupying different positions along the vacancy-hole axis, i.e., the $\langle 100 \rangle$ direction, producing the associated defects designated as the V_{Al}, V_F, V_{OH}, $[Li]^0$, $[Na]^0$, and $[K]^0$ centers.[4-7] (Of these, the first has been observed only in MgO, while the last has been produced in CaO and SrO only.) The properties of these centers have been investigated by both magnetic-resonance and optical-absorption techniques. Electron-nuclear double-resonance (ENDOR) measurements have established the positions of the impurity nuclei relative to the trapped hole for all of the above with the exception of K. In these systems, the $O^- - O^{2-}$ distance along the $\langle 100 \rangle$ direction deviates from the normal lattice spacing in proportion to the crystal-lattice constant a_0. ENDOR results have previously been reported for the V_{OD} center in deuterated MgO,[8] and CaO,[9] and the data indicated a similar linear variation. In this paper we report the production of the V_{OD} center in SrO single crystals and ENDOR measurements performed at 4.2 K which show that although the linear variation is true for hydrogen, it is not true for deuterium. Further, unlike the earlier cases where the axial relaxation was outward, the axial relaxation is inward for the SrO:V_{OD} defect.

II. EXPERIMENTAL

Single crystals of SrO were grown by the submerged-arc fusion process[10] using reagent-grade SrO powder supplied by the Mallinckrodt Chemical Corp. The hygroscopic single crystals from several growths were sealed in a container with D_2O and allowed to absorb the 100% deuterated water over a period of many weeks. These presoaked single crystals were used as starting materials in a final crystal growth in the arc furnace to yield the deuterated SrO single crystals. Following procedures previously described,[6] the V_{OD} centers were produced at 77 K by a short-duration γ irradiation from a ^{60}Co source and the samples were mounted cold into the ENDOR spectrometer without any intervening warmup. All magnetic field measurements were obtained with a proton nuclear-magnetic-resonance probe and the electronic- and nuclear-resonance frequencies were read directly by means of a Hewlett-Packard 5245L frequency counter with an HP model 5255A frequency converter.

III. RESULTS AND DISCUSSION

At 77 K, the EPR spectra revealed a defect possessing axial symmetry about the crystal $\langle 100 \rangle$ directions. The electronic g values agreed within experimental error with those previously reported for the V_{OH} center in SrO.[5,11] The spectral lines associated with this center do not exhibit resolved hyperfine structure at any orientation of the magnetic field. Upon cooling the sample to 4.2 K, the spectral lines, although narrowing in width, remained single. (At 4.2 K, the width of the line when the field orientation was parallel or perpend-

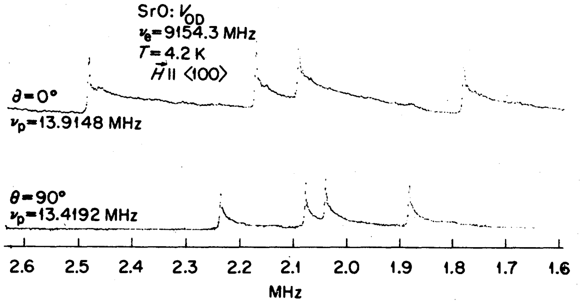

FIG. 1. ENDOR spectra of V_{OD} centers with the applied magnetic field parallel and perpendicular to the defect axis. Applied magnetic field is specified in terms of proton resonance frequency.

icular to the symmetry axis was ~0.6 and ~0.8 G, respectively, whereas at 77 K, the widths were ~0.9 and 1.6 G, respectively.) ENDOR experiments performed on these single EPR lines at 4.2 K yielded the spectra shown in Fig. 1., where the external magnetic field was directed along and perpendicular to the axis of symmetry of the center. The number of ENDOR lines fixes the spin of the nucleus involved at $I = 1$. At $\theta = 0°$, the average value of the ENDOR frequencies, which is equal in first order to the free nuclear Larmor frequency, unequivocally identifies the pertinent nucleus as deuterium. Figure 2 shows the ENDOR angular variation for the V_{OD} center with the magnetic field lying in a $\{100\}$ plane. From the deuterium identification and the angular variations, we conclude that the defect has ⟨100⟩ axial symmetry and possesses the linear configuration

$$OD^- \text{-(Sr vacancy)-} O^- .$$

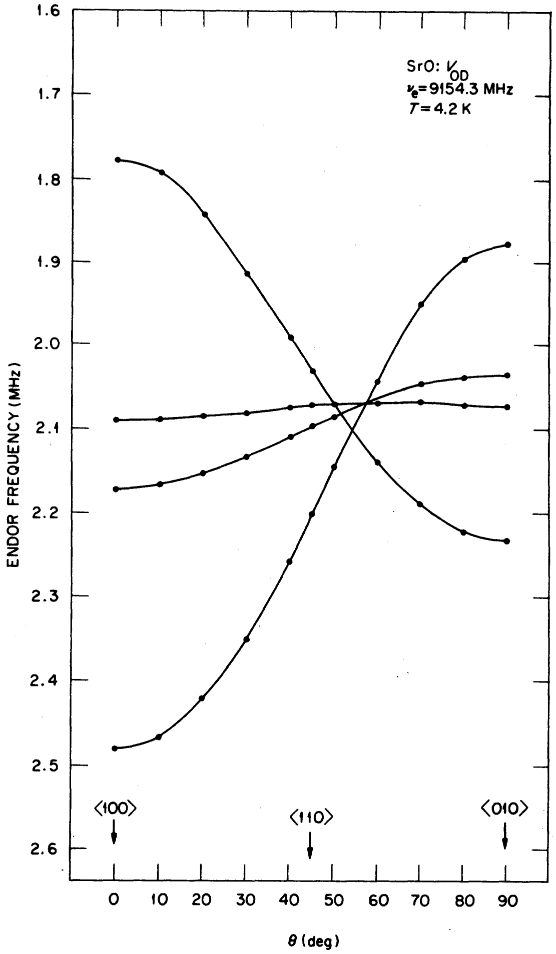

FIG. 2. Angular variation in the $\{100\}$ plane of the ENDOR for the SrO:V_{OD} center.

TABLE I. Spin-Hamiltonian parameters for trapped-hole centers.

	$g_{\parallel}$	$g_{\perp}$	$A_{\parallel}$ (MHz)	$A_{\perp}$ (MHz)	P (MHz)	Ref.
MgO:[Li]^0	2.0049(1)	2.0545(1)	+0.087(1)	−6.912(1)	−0.014(1)	6
CaO:[Li]^0	2.0020(1)	2.0891(1)	+0.161(1)	−3.846(1)	+0.009(1)	6
SrO:[Li]^0	2.0003(1)	2.0934(1)	+0.533(1)	−2.103(1)	+0.013(1)	6
MgO:[Na]^0	2.0057(4)	2.0725(4)	+3.024(2)	−11.259(2)	+0.790(1)	6
CaO:[Na]^0	2.0003(2)	2.1227(2)	−5.390(1)	−11.135(1)	+0.446(1)	6
SrO:[Na]^0	1.9955(4)	2.1454(4)	−5.115(2)	−8.391(2)	+0.245(1)	6
MgO:V_F	2.0032(2)	2.0390(2)	+2.114(2)	−0.687(2)	···	14
CaO:V_F	2.0017(2)	2.0719(2)	+1.553(2)	−0.461(2)	···	14
SrO:V_F	2.0014(3)	2.0736(3)	+1.065(3)	−0.465(3)	···	5
MgO:V_{OH}	2.0033(2)	2.0398(2)	+4.843(2)	−2.315(2)	···	14
CaO:V_{OH}	2.0018(2)	2.0729(2)	+2.758(2)	−1.385(2)	···	14
SrO:V_{OH}	2.0014(3)	2.0751(3)	+2.029(3)	−1.036(3)	···	5
MgO:V_{OD}			+0.734(5)	−0.356(5)	+0.173(8)	8
CaO:V_{OD}	2.0020(2)	2.0730(2)	+0.423(1)	−0.212(1)	+0.188(1)	9
SrO:V_{OD}	2.0013(2)	2.0751(3)	+0.396(1)	−0.195(1)	+0.158(1)	This work

The spectrum was described by the usual spin Hamiltonian

$$\mathcal{H}=\mu_B\left[g_{\parallel}H_zS_z+g_{\perp}(H_xS_x+H_yS_y)\right]+A_{\parallel}S_zI_z+A_{\perp}(S_xI_x+S_yI_y)+P\left[I_z^2-\tfrac{1}{3}I(I+1)\right]-g_N\mu_N\vec{\mathrm{H}}\cdot\vec{\mathrm{I}}\,, \tag{1}$$

with $S=\frac{1}{2}$ and $I=1$. The experimental data were fed into a computer and a direct diagonalization of $\mathcal{H}$ yielded a least-squares best fit to determine the seven parameters $g_{\parallel}$, $g_{\perp}$, $A_{\parallel}$, $A_{\perp}$, P, $(g_N)_{\parallel}$, and $(g_N)_{\perp}$. As expected, the last two parameters were found to be equal and identical to the value quoted in the nuclear data tables.[12] The final results for the electronic g values, $g_{\parallel}=2.0013(2)$ and $g_{\perp}=2.0751(3)$, are in accord with the earlier ENDOR results on the V_{OH} center in SrO.[5,11] The parameters are shown in Table I, where similar data obtained earlier for the V_{OD} center in[8] MgO and[9] CaO are also listed. Relative signs of the parameters follow from the ENDOR measurements and the absolute signs are fixed by the reported positive sign of the deuteron nuclear magnetic moment.[12]

Following Schirmer,[13] the spin-Hamiltonian magnetic hyperfine interaction parameters $A_{\parallel}$ and $A_{\perp}$ were decomposed into the isotropic and anisotropic parameters a and b, where

$$A_{\parallel}=a+2b,\quad A_{\perp}=a-b(1+\tfrac{1}{2}\Delta g_{\perp})\,, \tag{2}$$

and $\Delta g_{\perp}=g_{\perp}-2.002\,32$. These values are listed in Table II. Assuming that the anisotropic portion of the hyperfine interaction b arises from a purely classical dipole-dipole interaction,

$$b=\mu_e\,\mu_D/hIS\langle R^3\rangle\,, \tag{3}$$

where R is the distance of the deuterium from the trapped hole (O^- ion) and b is measured in Hz. A more realistic value of the compensator distance l, which takes into account the finite extent of the trapped-hole wave function in terms of its average square radius $\langle\rho^2\rangle$, may be obtained with the formula[13]

$$\frac{1}{\langle R^3\rangle}=\frac{1}{l^3}+\frac{12}{5}\frac{\langle\rho^2\rangle}{l^5}\,. \tag{4}$$

Following the procedure employed earlier,[5,6,14] two values of l were calculated from the two extreme values of $\langle\rho^2\rangle$ (0.48 and 0.85 Å^2) used by Schirmer[13] and the average value $\bar{l}$ was adopted as more representative of the distance between the deuterium nucleus and the O^- ion. Adding the expected OD^- bond length to the $\bar{l}$ value yields the axial O^-–O^{2-} distance d. (Here the OD^- ion is considered as $O^{2-}D^+$.) The values R, $\bar{l}$, and d obtained in this way for the SrO:V_{OD} center are listed in Table II along with the corresponding values for the other V_{OH} and V_{OD} centers reported earlier. (In this table, the OH^- and OD^- bond lengths were taken to be 0.98 and 0.99 Å, respectively.[15]) Figure 3 is a graph of d versus the lattice constant a_0 for the V_{OH} and V_{OD} centers in MgO, CaO, and SrO. It can be seen that if one considers V_{OD} centers in MgO and CaO, the points fall on the same straight line determined by the V_{OH} data in all three hosts. However, the V_{OD} point for SrO does *not* fall on that straight line and, in fact, lies *below* the $d=a_0$ line, implying an inward relaxation of the O^-–O^{2-} distance relative to the undistorted O^{2-}–O^{2-} distance.

The isotropic hyperfine parameter a is directly

TABLE II. Decomposition of magnetic hyperfine interaction: l_1 calculated for $\rho^2=0.48$, l_2 calculated for $\rho^2=0.85$, $\bar{l}$ average of l_1 and l_2. For references , see Table I.

	a (MHz)	b (MHz)	R (Å)	l_1 (Å)	l_2 (Å)	$\bar{l}$ (Å)	d (Å)	$\lvert\psi(0)\rvert^2$ (10^{20} cm^{-3})	$d-a_0$ (Å)
MgO:$[\mathrm{Li}]^0$	−4.539	+2.313	2.368	2.505	2.588	2.547	4.547	−176.4	+0.334
CaO:$[\mathrm{Li}]^0$	−2.472	+1.317	2.858	2.977	3.053	3.015	5.015	−96.1	+0.200
SrO:$[\mathrm{Li}]^0$	−1.198	+0.866	3.287	3.393	3.463	3.428	5.428	−46.6	+0.268
MgO:$[\mathrm{Na}]^0$	−6.388	+4.706	1.644	1.817	1.908	1.863	4.213	−364.5	0.0
CaO:$[\mathrm{Na}]^0$	−9.145	+1.877	2.234	2.376	2.461	2.419	4.769	−521.9	−0.046
SrO:$[\mathrm{Na}]^0$	−7.248	+1.067	2.697	2.821	2.900	2.861	5.211	−413.6	+0.051
MgO:V_{F}	+0.258	+0.928	4.312	4.396	4.455	4.426	4.426	+4.1	+0.213
CaO:V_{F}	+0.226	+0.664	4.821	4.897	4.951	4.925	4.925	+3.6	+0.110
SrO:V_{F}	+0.055	+0.504	5.282	5.352	5.402	5.377	5.377	+0.9	+0.217
MgO:V_{OH}	+0.101	+2.371	3.219	3.327	3.398	3.362	4.342	+1.5	+0.129
CaO:V_{OH}	+0.028	+1.365	3.869	3.961	4.025	3.993	4.973	+0.4	+0.158
SrO:V_{OH}	+0.011	+1.009	4.279	4.364	4.423	4.394	5.374	+0.2	+0.214
MgO:V_{OD}	+0.012	+0.361	3.227	3.335	3.407	3.372	4.362	+1.2	+0.149
CaO:V_{OD}	+0.005	+0.209	3.872	3.965	4.028	3.997	4.987	+0.5	+0.172
SrO:V_{OD}	+0.007	+0.195	3.965	4.056	4.118	4.088	5.078	+0.7	−0.082

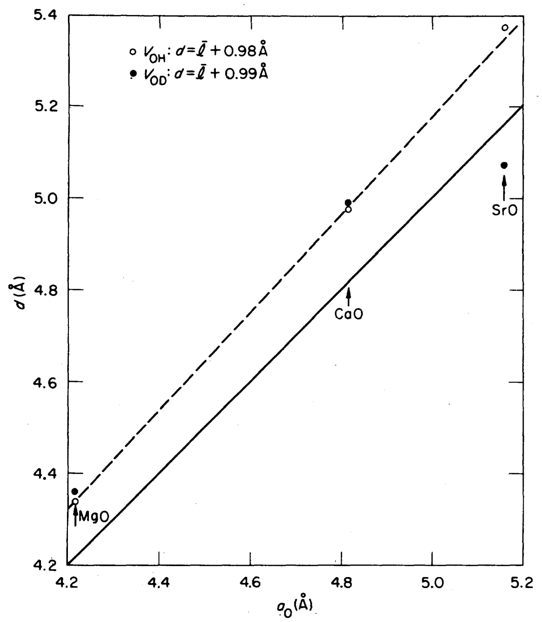

FIG. 3. Graph of $O^{-}-O^{2-}$ distance as a function of the lattice constant. Distances were calculated from the dipole interaction and the OH^{-} (OD^{-}) bond length. The solid line represents $d=a_0$.

proportional to the probability density $|\psi(0)|^2$ at the nucleus, and these values are also shown in Table II. Although the $|\psi(0)|^2$ for the V_{OH} and V_{OD} centers differ by 20 and 25% in MgO and CaO, respectively, these values differ by 250% in SrO. The normal expectation would be for $|\psi(0)|^2$ to gradually decrease as one proceeds from MgO to the more open SrO lattice. Generally for hydrogen and deuterium, this has been found to be true except for the SrO:V_{OD} case. Here the relatively large value found for $|\psi(0)|^2$ is consistent with the inward relaxation discussed above.

Figure 4 exhibits the intensity of the V_{OD} EPR signals at ~90 K following a series of 5-min isochronal anneals at each point shown. Although the decay temperature (defined as the temperature at which one-half of the centers have annealed out) of ~235 K is higher than the 195-K value reported earlier for the SrO:V_{OH} center,[5] caution must be taken in making comparisons of annealing temperatures. The concentrations of other defects and impurities, which can trap holes, may vary from sample to sample, and therefore affect the annealing temperature.

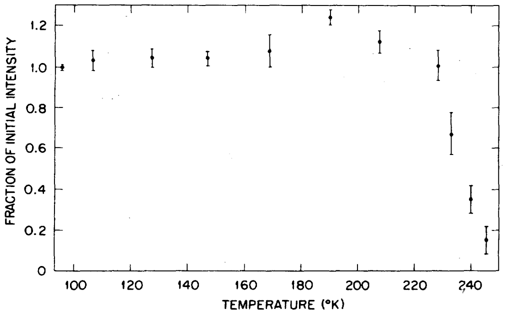

FIG. 4. Isochronal (5 min) annealing of V_{OD} centers in SrO.

Our samples contain many other defects in addition to the axial V_{OD} center. The complete EPR spectrum obtained at 4.2 K with $\vec{H}$ along a ⟨100⟩ axis is shown in Fig. 5. Although we could not follow the angular variation of all the lines, we were able to observe deuterium ENDOR responses for both of the lines arbitrarily labeled as A in Fig. 5. Each of these two A lines is actually a superposition of at least four lines which split and move toward the center of the spectrum when the magnetic field is rotated in a {100} plane. In the ⟨100⟩ direction, ENDOR responses were found at 1.922, 1.721, 1.666, and 1.464 MHz for the low-field line, while for the high-field A line, responses were found at 2.656, 2.459, 2.402, and 2.206 MHz. The values of the deuteron magnetic resonance frequency at the two fields were 1.563 and 2.558 MHz, respectively. Their average, 2.060 MHz, is in good agreement with the average of the eight ENDOR frequencies, 2.062 MHz. This comparison minimizes frequency shifts due to second-order hyperfine effects. Similarly, deuterium ENDOR signals were also observed on the lines labeled G and H in Fig. 5. Attempts to follow the angular variation of the EPR lines were unsuccess-

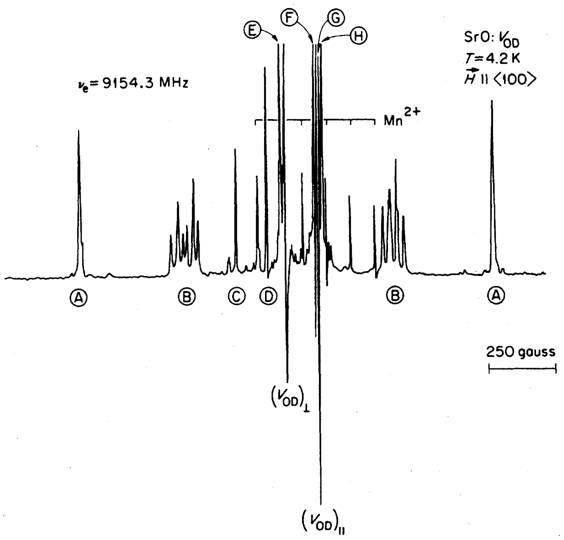

FIG. 5. EPR spectrum for deuterated SrO single crystal with $\vec{H}$ ∥ ⟨100⟩. Letters represent arbitrary labeling of lines.

ful, however, owing to the weak intensity of the individual component lines when they were no longer superimposed as in Fig. 5.

Among several other defects created by the irradiation process, we were able to observe a ⟨111⟩ axial center previously reported in both potassium[7] and hydrogen[5,16] doped SrO crystals. Although either of the two molecular ions, $(OH)^{2-}$ and $(OF)^{2-}$, could conceivably be responsible for this defect, since both hydrogen and fluorine were detected, we indicated[16] that the latter ion appears to be a better candidate, by analogy with the situation in MgO.[17,18] Deuterium is the predominant impurity in the crystals used for the present study. To be sure, these deuterated crystals do contain hydrogen and fluorine, since we have observed low-intensity ENDOR signals due to these nuclei in accompanying V_{OH} and V_F centers. If this axial ⟨111⟩ defect were indeed due to hydrogen, we would expect to observe a sizable EPR signal from the deuterium analog. No such signals were observed. Therefore, we have no reason at this time to alter our previous assignment of this center to a fluorine- rather than a hydrogen-associated defect. The identity of the impurity as well as the model configuration for this defect cannot be determined without further experiments, such as ENDOR. (It should be noted that upon cooling from 77 to 4.2 K, the EPR signals for the ⟨111⟩ center are drastically reduced in relative intensity. Therefore, the signals are probably due to a resonance which is not in the ground state.)

In summary, for comparison, convenience, and completeness, in Table II we have tabulated ENDOR data obtained previously for the impurity-associated trapped-hole centers in the alkaline-earth oxides. The accompanying decomposition of the magnetic hyperfine interaction performed in the manner outlined above is shown in Table II. For all the cases shown in Table II, with the exception of deuterium, plots of d versus a_0 yield essentially straight lines within experimental error.[5,6] Regardless of the method of analyzing the data and the admitted uncertainty in the resultant values of d, it is apparent that the deuterium case in SrO is definitely different from the other systems. Our derived value of 5.078 Å for the oxygen-oxygen spacing in the SrO:V_{OD} system is smaller than the normal oxygen spacing of 5.16 Å for the undisturbed lattice. Such an inward relaxation is contrary to the previously observed cases of impurity-associated trapped-hole centers in the alkaline-earth oxides where outward distortions from the normal lattice spacing generally occur. This difference in distortion between hydrogen and deuterium in SrO must be associated with a vibrational behavior, since essentially only mass distinguishes the two cases. The fact that the Sr ionic radius is larger than the Mg or Ca radii allows more room for the vacancy and apparently permits this isotopic effect to manifest itself in SrO.

ACKNOWLEDGMENT

We are grateful to F. A. Modine for a critical reading of the manuscript.

---

*On leave from Instituto de Fisica, U.N.A.M., Mexico, D. F.

†Research sponsored by Energy Research Development Administration under contract with Union Carbide Corp.

‡On sabbatical leave from University of Illinois, Urbana, Ill.

[1] Y. Chen and M. M. Abraham, New Phys. (Seoul) 15, 47 (1975).

[2] A. E. Hughes and B. Henderson, *Defects in Crystalline Solids*, edited by J. H. Crawford, Jr. and L. M. Slifkin (Plenum, New York, 1972).

[3] B. Henderson and J. E. Wertz, Adv. Phys. 17, 749 (1968).

[4] W. P. Unruh, Y. Chen, and M. M. Abraham, Phys. Rev. Lett. 30, 446 (1973); M. M. Abraham, Y. Chen, and W. P. Unruh, Phys. Rev. B 9, 1842 (1974).

[5] M. M. Abraham, Y. Chen, and J. Rubio O., Phys. Rev. B 14, 2603 (1976), and references therein.

[6] M. M. Abraham, W. P. Unruh, and Y. Chen, Phys. Rev. B 10, 3540 (1974), and references therein.

[7] M. M. Abraham, Y. Chen, J. T. Lewis, and F. A. Modine, Phys. Rev. B 7, 2732 (1973).

[8] B. Henderson, J. L. Kolopus, and W. P. Unruh, J. Chem. Phys. 55, 3519 (1971).

[9] M. M. Abraham, Y. Chen, and W. P. Unruh, Phys. Rev. B 12, 4766 (1975).

[10] M. M. Abraham, C. T. Butler, and Y. Chen, J. Chem. Phys. 55, 3752 (1971).

[11] W. B. Blake, H. A. Gitelson, and J. E. Wertz, J. Phys. C 4, 261 (1971).

[12] G. H. Fuller and V. W. Cohen, Nucl. Data Tables A 5, 433 (1969).

[13] O. F. Schirmer, J. Phys. Chem. Solids 32, 499 (1971).

[14] W. P. Unruh, Y. Chen, and M. M. Abraham, J. Chem. Phys. 59, 3284 (1973), and references therein.

[15] W. R. Busing and H. A. Levy, J. Chem. Phys. 26, 563 (1957); H. G. Smith (private communication).

[16] J. Rubio O., H. T. Tohver, Y. Chen, and M. M. Abraham, Phys. Rev. B 14, 5466 (1976).

[17] G. Rius and R. T. Cox, Phys. Lett. A 27, 76 (1968).

[18] G. Rius, R. T. Cox, P. Freund, and J. Owen, J. Phys. C 7, 581 (1974).